

# Maximal Decay Rate and Optimal Sensor Feedback Amplifiers for Fast Stabilization of Magnetizable Piezoelectric Beam Equations

Ahmet Özkan Özer<sup>1</sup>, Rafi Emran<sup>1</sup> and Ahmet Kaan Aydın<sup>2</sup>

**Abstract**—The fully dynamic PDE model, describing the longitudinal oscillations on magnetizable piezoelectric beams, with two boundary feedback controllers is known to have exponentially stable solutions. Finding the maximal decay rate and optimal feedback sensor amplifiers are crucial for the fast suppression of oscillations on these beams. In this paper, a Lyapunov-based approach is adopted to obtain a maximal decay rate with (i) two separate sensor feedback amplifiers for exact exponential stabilization and (ii) a unique feedback amplifier for the simultaneous exponential stabilization. For case (i), feedback amplifiers come out of an optimization process where the safe range of amplifiers are explicitly determined in terms of material constants to achieve the fastest exponential decay rate possible. It is also shown that for certain material parameter combinations, feedback amplifiers may not exist. The case (ii) is a special case of case (i), and a safe range of amplifiers can also be established. However, for a wider class of realistic material parameters the feedback amplifiers can not be established to achieve the desired maximal decay rate. To show the strength of our results, several numerical experiments are provided.

## I. INTRODUCTION

Consider a beam of magnetizable piezoelectric material, clamped on one side and free to oscillate on the other, with the addition of a sensor for the tip velocity and another one for the tip current. The beam is of length  $L$  and thickness  $h$ . Assume that the transverse oscillations of the beam are negligible, so the longitudinal vibrations, in the form of expansion and compression of the center line of the beam, are the only oscillations of note. Even though electrostatic/quasi-static models accurately represents the overall dynamics [7] for non-magnetizable piezoelectric beams, dynamic effects due to the electromagnetic field for (acoustic) magnetizable piezoelectric beams are pronounced and must be taken into account in the modeling [3], [11]. Denoting  $v(x, t)$  and  $p(x, t)$  by the longitudinal oscillations of the center line of the beam and the total charge accumulated at the electrodes of the beam, respectively, see Fig 1, the equations of motion is a system of partial differential equations [3] as the following

$$\begin{cases} \begin{pmatrix} \rho & 0 \\ 0 & \mu \end{pmatrix} \begin{bmatrix} v_{tt} \\ p_{tt} \end{bmatrix} - \begin{pmatrix} \alpha & -\gamma\beta \\ -\gamma\beta & \beta \end{pmatrix} \begin{bmatrix} v_{xx} \\ p_{xx} \end{bmatrix} = \begin{bmatrix} 0 \\ 0 \end{bmatrix}, \end{cases} \quad (1)$$

$$\begin{cases} v(0, t) = p(0, t) = 0, \\ \begin{pmatrix} \alpha & -\gamma\beta \\ -\gamma\beta & \beta \end{pmatrix} \begin{bmatrix} v_x \\ p_x \end{bmatrix} (L, t) = \begin{bmatrix} u_1(t) \\ u_2(t) \end{bmatrix}, \quad t \in \mathbb{R}^+ \end{cases} \quad (2)$$

$$[v, p, v_t, p_t](x, 0) = [v_0, p_0, v_1, p_1](x), \quad x \in [0, L] \quad (3)$$

<sup>1</sup>Department of Mathematics, Western Kentucky University, Bowling Green, KY 42101, USA. ozkan.ozer@wku.edu mdrasias.sadeqibnemran227@topper.wku.edu

<sup>2</sup>Department of Mathematics, University of Maryland, Baltimore County, Baltimore, MD 21250, USA. aaydin1@umbc.edu

where  $\rho$ ,  $\alpha$ ,  $\beta$ ,  $\gamma$ , and  $\mu$  are the mass density per unit volume, the elastic stiffness, the impermeability, the piezoelectric constant, and the magnetic permeability, respectively, and  $g(t)$  and  $V(t)$  are strain and voltage actuators.

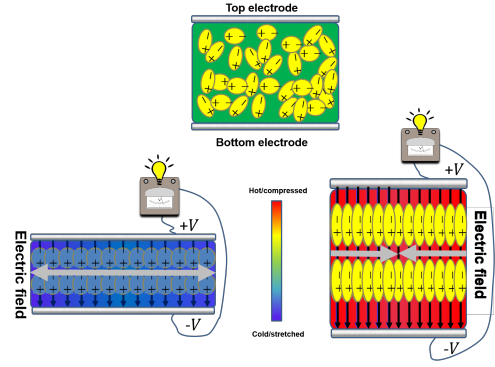


Fig. 1. (Top) A piezoelectric beam is an elastic beam with electrodes at their top and bottom surfaces, and connected to an external electric circuit. As voltage is applied to its electrodes, it actively (Bottom-left) stretches or (Bottom-right) compresses in the longitudinal directions. Magnetic effects (stored/produced) have a direct contribution to the beam vibrations and the electric field across the electrodes.

Defining  $\alpha_1 := \alpha - \gamma^2\beta > 0$ , and the following constants

$$\begin{aligned} \zeta_1 &= \frac{1}{\sqrt{2}} \sqrt{\frac{\alpha\mu}{\alpha_1\beta} + \frac{\rho}{\alpha_1} + \sqrt{\left(\frac{\alpha\mu}{\alpha_1\beta} + \frac{\rho}{\alpha_1}\right)^2 - \frac{4\rho\mu}{\beta\alpha_1}}} \\ \zeta_2 &= \frac{1}{\sqrt{2}} \sqrt{\frac{\alpha\mu}{\alpha_1\beta} + \frac{\rho}{\alpha_1} - \sqrt{\left(\frac{\alpha\mu}{\alpha_1\beta} + \frac{\rho}{\alpha_1}\right)^2 - \frac{4\rho\mu}{\beta\alpha_1}}} \end{aligned} \quad (4)$$

the natural energy of the solutions is defined as

$$E(t) = \frac{1}{2} \int_0^L \left[ \rho |v_t|^2 + \mu |p_t|^2 + \alpha_1 |v_x|^2 + \beta |\gamma v_x - p_x|^2 \right] dx. \quad (5)$$

The observability result for the model (1)-(3) with  $\xi_1, \xi_2 = 0$  and with only one sensor is not possible [3]. Considering two sensors,  $v_t(L, t)$  and  $p_t(L, t)$  being the sensor measurements for tip velocity sensor and total current accumulated at the electrodes of the piezoelectric beam, an observability result with a suboptimal observation time is proved [10]. Later, the same result is refined with the optimal observation time:

**Theorem 1.** [9, Theorem 2.2] Consider the weak solutions of the control-free system (1)-(3), i.e.  $\xi_1 = \xi_2 = 0$ , in the energy space. For any  $T > \frac{2L}{\eta}$  with  $\eta = \max(\zeta_1, \zeta_2)$ , there exists a constant  $C(T) > 0$  such that

$$\int_0^T \left( \rho |v_t(L, t)|^2 + \mu |p_t(L, t)|^2 \right) dt \geq C(T) E(0) \quad (6)$$

for all initial data  $[v_0, p_0, v_1, p_1](x)$  in the energy space.

The same sensor signals may be amplified and fed back to (1)-(3). The range of amplification depends on the limits of these sensors. Parallel to the observability result, it is known that even though only one sensor feedback may be enough to make the energy dissipative it is not enough to exponentially stabilize the system (1)-(3). The reason is that the closed-loop system with this type of control design only puts stringent conditions on the stabilization results [3]. Indeed, for a large class of material parameters exponential stability is at stake, and only for a small class of material parameters, the exponential stability can be achieved [4].

Consider two major cases for the choice of two sensor feedback for the design of actuators in (1)-(3). In the first case, different feedback amplifiers (gains),  $\xi_1, \xi_2 > 0$  are considered for each sensor feedback. In the other case, only one sensor feedback amplifier  $\xi_3 > 0$  is chosen for both actuators.

$$\text{Case I: } \begin{bmatrix} u_1(t) \\ u_2(t) \end{bmatrix} = - \begin{bmatrix} \xi_1 & 0 \\ 0 & \xi_2 \end{bmatrix} \begin{bmatrix} \dot{v}(L, t) \\ \dot{p}(L, t) \end{bmatrix}, \quad (7)$$

$$\text{Case II: } \begin{bmatrix} u_1(t) \\ u_2(t) \end{bmatrix} = - \begin{bmatrix} \xi_3 & 0 \\ 0 & \xi_3 \end{bmatrix} \begin{bmatrix} \dot{v}(L, t) \\ \dot{p}(L, t) \end{bmatrix}. \quad (8)$$

Case I leads to the ‘‘exact’’ exponential stability and it is only studied thoroughly in [10]. It is shown that the solutions of the controlled system (1)-(3) is exponentially stable. However, the proof is based on a decomposition of the system (1)-(3),(7) into a conservative system with nonzero initial conditions and a dissipative system with zero initial conditions. The exponential stability result follows from an observability inequality with a suboptimal observation time. Moreover, this approach neither provides an explicit description of a maximal decay rate nor optimal feedback amplifiers to achieve a maximal decay rate. Case II is a special case of Case I where a single feedback amplifier is used for both sensor measurements to achieve a simultaneous exponential stabilization. It is more restrictive for the choice of amplifier but practical in applications.

The first goal in this paper is to prove the existence of the maximal decay rate for (1)-(3) with each case (7)-(8). Once this is obtained by a Lyapunov-based approach, optimality and safe range for each feedback amplifier  $\xi_1, \xi_2$  and  $\xi_3$  are established to achieve the maximal decay rate for any type of initial conditions in the energy space. Finally, a recently developed model reduction by Finite Differences [9] of the model (1)-(3) is being used to show the strengths of our analysis.

## II. EXPONENTIAL STABILITY RESULT

In order for solutions of the system (1)-(3) to stabilize exponentially, the energy must be dissipative first. The proof is omitted.

**Theorem 2.** For all  $t > 0$ , the energy  $E(t)$  in (5) is dissipative with each case in (7)-(8):

$$\text{Case I: } \frac{dE}{dt} = -\xi_1 |\dot{v}(L, t)|^2 - \xi_2 |\dot{p}(L, t)|^2 \leq 0.$$

$$\text{Case II: } \frac{dE}{dt} = -\xi_3 \left( |\dot{v}(L, t)|^2 + |\dot{p}(L, t)|^2 \right) \leq 0.$$

Now, define an energy-like functional  $F(t)$  in order to define a perturbed energy functional  $E_\delta(t)$  as the following

$$\begin{aligned} F(t) &:= \int_0^L (\rho v_t x v_x + \mu p_t x p_x) dx, \\ E_\delta(t) &:= E(t) + \delta F(t), \end{aligned} \quad (9)$$

where  $\delta > 0$  will be determined as a function of sensor feedback amplifiers  $\xi_1, \xi_2, \xi_3$  later.

The following two lemmas for  $F(t)$  and  $E_\delta(t)$  are needed to prove our main exponential stability result. Let

$$\eta := \max \left( \sqrt{\frac{\rho}{\alpha_1}} + \sqrt{\frac{\mu\gamma^2}{\alpha_1}}, \sqrt{\frac{\mu}{\beta}} + \sqrt{\frac{\mu\gamma^2}{\alpha_1}} \right). \quad (10)$$

**Lemma 1.** Letting  $0 < \delta < \frac{1}{\eta L}$ , for all  $t > 0$  and  $\delta > 0$ ,  $E_\delta(t)$  in (9) is equivalent to  $E(t)$  in (5), i.e.

$$(1 - \delta\eta L) E(t) \leq E_\delta(t) \leq (1 + \delta\eta L) E(t). \quad (11)$$

*Proof.* By the Hölder’s, Minkowski’s, Triangle inequalities, as well as algebraic manipulations,  $F(t)$  satisfies

$$\begin{aligned} |F(t)| &= \left| \int_0^L (\rho v_t x v_x + \mu p_t x p_x) dx \right| \\ &\leq L \left[ \left( \int_0^L \rho |v_t|^2 \right)^{\frac{1}{2}} \left( \frac{\rho}{\alpha_1} \int_0^L \alpha_1 |v_x|^2 \right)^{\frac{1}{2}} \right. \\ &\quad \left. + \left( \int_0^L \mu |p_t|^2 \right)^{\frac{1}{2}} \left( \int_0^L \mu |\gamma v_x - p_x|^2 dx \right)^{\frac{1}{2}} \right. \\ &\quad \left. + \left( \mu \int_0^L \gamma^2 |v_x|^2 dx \right)^{\frac{1}{2}} \right] \\ &\leq \frac{L}{2} \left[ \sqrt{\frac{\rho}{\alpha_1}} \int_0^L \rho |v_t|^2 + \left( \sqrt{\frac{\rho}{\alpha_1}} + \sqrt{\frac{\mu\gamma^2}{\alpha_1}} \right) \int_0^L \alpha_1 |v_x|^2 \right. \\ &\quad \left. + \left( \sqrt{\frac{\mu}{\beta}} + \sqrt{\frac{\mu\gamma^2}{\alpha_1}} \right) \int_0^L \mu |p_t|^2 + \sqrt{\frac{\mu}{\beta}} \int_0^L \beta |\gamma v_x - p_x|^2 \right] \\ &\leq L\eta E(t). \end{aligned}$$

Since  $F(t) \leq \eta L E(t)$ , this leads to

$$|E_\delta(t)| \leq |E(t)| + \delta |F(t)| \leq (1 + \eta\delta L) E(t),$$

and analogously,  $|E_\delta(t)| \geq (1 - \eta\delta L) E(t)$ , and therefore, (11) is immediate  $\square$

**Lemma 2.** For any  $\epsilon, t > 0$ ,  $F(t)$  in (9) satisfies the following inequalities for Cases I and II, respectively,

$$\begin{aligned} \frac{dF}{dt} &\leq -E(t) + \frac{L}{2} \left[ \rho + \frac{(1 + \epsilon)\xi_1^2}{\alpha_1} \right] |v_t(L, t)|^2 \\ &\quad + \frac{L}{2} \left[ \mu + \left( 1 + \frac{1}{\epsilon} \frac{\xi_2^2 \gamma^2}{\alpha_1} + \frac{\xi_2^2}{\beta} \right) \right] |p_t(L, t)|^2, \end{aligned} \quad (12)$$

$$\begin{aligned} \frac{dF}{dt} &\leq -E(t) + \frac{L}{2} \left[ \rho + \frac{(1 + \epsilon)\xi_3^2}{\alpha_1} \right] |v_t(L, t)|^2 \\ &\quad + \frac{L}{2} \left[ \mu + \left( 1 + \frac{1}{\epsilon} \frac{\xi_3^2 \gamma^2}{\alpha_1} + \frac{\xi_3^2}{\beta} \right) \right] |p_t(L, t)|^2. \end{aligned} \quad (13)$$

*Proof.* Recalling  $\alpha_1 = \alpha - \gamma^2\beta$ , and (1),

$$\begin{aligned} \frac{dF}{dt} &= \int_0^L \rho (v_{tt} x v_x + v_t x v_{xt}) + \mu (p_{tt} x p_x + p_t x p_{xt}) dx \\ &= \frac{L}{2} \beta (\gamma v_x(L, t) - p_x(L, t))^2 + \frac{L}{2} \alpha_1 (v_x(L, t))^2 \\ &\quad + \frac{L}{2} \left[ \rho |v_t(L, t)|^2 + \mu |p_t(L, t)|^2 \right] - E(t). \end{aligned}$$

Next, the boundary conditions (2) are used so that

$$\begin{aligned} \text{Case I: } \frac{dF}{dt} &= -E(t) + \frac{L}{2} \left( \mu + \frac{\xi_2^2}{\beta} \right) |p_t(L, t)|^2 \\ &+ \frac{L\rho}{2} |v_t(L, t)|^2 + \frac{L}{2\alpha_1} (\xi_1 |v_t(L, t)| + \xi_2 \gamma |v_t(L, t)|)^2, \\ \text{Case II: } \frac{dF}{dt} &= -E(t) + \frac{L}{2} \left( \mu + \frac{\xi_3^2}{\beta} \right) |p_t(L, t)|^2 \\ &+ \frac{L\rho}{2} |v_t(L, t)|^2 + \frac{L}{2\alpha_1} (\xi_3 |v_t(L, t)| + \xi_3 \gamma |v_t(L, t)|)^2. \end{aligned}$$

Finally, by the Young's inequality, (12) and (13) is obtained for any  $\epsilon > 0$ .  $\square$

Now, the exponential stability result is takes the following form

**Theorem 3.** *The energy  $E(t)$  of solutions decays exponentially, i.e.*

$$\begin{aligned} E(t) &\leq ME(0)e^{-\sigma t}, \quad \forall t > 0 \\ \sigma(\delta) &= \delta(1 - \delta L\eta), \quad M(\delta) = \frac{1 + \delta L\eta}{1 - \delta L\eta}, \end{aligned} \quad (14)$$

where  $\delta$  for each case is

$$\begin{aligned} \text{Case I: } \left\{ \begin{array}{l} \delta_{\text{I}}(\xi_1, \xi_2, \epsilon) := \frac{1}{2L} \min\left(\frac{1}{\eta}, f_1, f_2\right), \\ f_1(\xi_1, \epsilon) := \frac{2\xi_1\alpha_1}{\rho\alpha_1 + (1+\epsilon)\xi_1^2}, \\ f_2(\xi_2, \epsilon) := \frac{2\xi_2\epsilon\alpha_1\beta}{\epsilon\mu\alpha_1\beta + (\epsilon\alpha + \gamma^2\beta)\xi_2^2}. \end{array} \right. & (15) \\ \text{Case II: } \left\{ \begin{array}{l} \delta_{\text{II}}(\xi_3, \epsilon) := \frac{1}{2L} \min\left(\frac{1}{\eta}, g_1, g_2\right), \\ g_1(\xi_3, \epsilon) = \frac{2\xi_3\alpha_1}{\rho\alpha_1 + (1+\epsilon)\xi_3^2}, \\ g_2(\xi_3, \epsilon) = \frac{2\xi_3\epsilon\alpha_1\beta}{\epsilon\mu\alpha_1\beta + (\epsilon\alpha + \gamma^2\beta)\xi_3^2}. \end{array} \right. & (16) \end{aligned}$$

*Proof.* Since  $\frac{dE_\delta}{dt} = \frac{dE}{dt} + \delta \frac{dF}{dt}$ , by Lemma 2 and a direct calculation lead to

$$\begin{aligned} \text{Case I: } \frac{dE_\delta}{dt} &\leq \underbrace{\left[ \frac{\delta_{\text{I}}L}{2} \left[ \rho + \frac{(1+\epsilon)\xi_1^2}{\alpha_1} \right] - \xi_1 \right]}_{\leq 0} |v_t(L, t)|^2 \\ &+ \underbrace{\left[ \frac{\delta_{\text{I}}L}{2} \left[ \mu + \frac{(\epsilon\alpha + \gamma^2\beta)\xi_2^2}{\epsilon\alpha_1\beta} \right] - \xi_2 \right]}_{\leq 0} |p_t(L, t)|^2 - \delta_{\text{I}}E(t) \end{aligned}$$

where  $\delta_{\text{I}}$  is chosen to make the coefficients nonpositive, i.e.

$$\delta_{\text{I}} \leq \frac{1}{2L} \min\left(\frac{1}{\eta}, f_1(\xi_1, \epsilon), f_2(\xi_2, \epsilon)\right). \quad (17)$$

$$\begin{aligned} \text{Case II: } \frac{dE_\delta}{dt} &\leq \underbrace{\left[ \frac{\delta_{\text{II}}L}{2} \left[ \rho + \frac{(1+\epsilon)\xi_3^2}{\alpha_1} \right] - \xi_3 \right]}_{\leq 0} |v_t(L, t)|^2 \\ &+ \underbrace{\left[ \frac{\delta_{\text{II}}L}{2} \left[ \mu + \frac{(\epsilon\alpha + \gamma^2\beta)\xi_3^2}{\epsilon\alpha_1\beta} \right] - \xi_3 \right]}_{\leq 0} |p_t(L, t)|^2 - \delta_{\text{II}}E(t) \end{aligned}$$

where  $\delta_{\text{II}}$  is chosen to make the coefficients nonpositive, i.e.

$$\delta_{\text{II}} \leq \frac{1}{2L} \min\left(\frac{1}{\eta}, g_1(\xi_3, \epsilon), g_2(\xi_3, \epsilon)\right). \quad (18)$$

Next, for both cases, by the equivalence of  $E(t)$  and  $E_\delta(t)$  from Lemma 1,

$$\frac{dE_\delta}{dt} \leq -\delta(1 - \delta L\eta) E_\delta(t). \quad (19)$$

By choosing  $\sigma = \delta(1 - \delta L\eta) > 0$ , together with (19) lead to

$$E_\delta(t) \leq E_\delta(0)e^{-\sigma t}. \quad (20)$$

Hence, (20) together with Lemma 1 lead to

$$E(t) \leq \frac{1 + \delta L\eta}{1 - \delta L\eta} e^{-\sigma t} E(0). \quad (21)$$

This concludes the proof.  $\square$

### III. OPTIMALITY OF SENSOR FEEDBACK AMPLIFIERS

The decay rate  $\sigma$  in Theorem 3 is maximal as the system exponentially stabilizes fastest. The  $\sigma$  is a function of  $\delta$ , and for both cases,  $\sigma$  makes its maximal value

$$\sigma_{\max}(\delta) = \frac{1}{4\eta L} \text{ achieved at } \delta = \frac{1}{2\eta L}. \quad (22)$$

Since  $\delta$  and  $\sigma$  are all functions of  $\epsilon$  and the sensor feedback amplifiers  $\xi_1, \xi_2, \xi_3$  in (7), the following results provide safe intervals for the feedback amplifiers and  $\epsilon$  to make sure that the maximal decay rate (22) is attained.

**Theorem 4.** *[Case I] Define non-negative constants*

$$\begin{aligned} c_1 &:= \frac{\alpha_1\eta - \sqrt{\alpha_1^2\eta^2 - (1+\epsilon)\rho\alpha_1}}{1+\epsilon}, \\ c_2 &:= \frac{\alpha_1\eta + \sqrt{\alpha_1^2\eta^2 - (1+\epsilon)\rho\alpha_1}}{1+\epsilon}, \\ c_3 &:= \frac{\epsilon\alpha_1\beta\eta - \sqrt{(\epsilon\alpha_1\beta\eta)^2 - (\epsilon\alpha + \beta\gamma^2)\epsilon\mu\alpha_1\beta}}{\epsilon\alpha + \beta\gamma^2}, \\ c_4 &:= \frac{\epsilon\alpha_1\beta\eta + \sqrt{(\epsilon\alpha_1\beta\eta)^2 - (\epsilon\alpha + \beta\gamma^2)\epsilon\mu\alpha_1\beta}}{\epsilon\alpha + \beta\gamma^2}, \end{aligned}$$

with any  $\epsilon$  such that

$$0 < \frac{\beta\gamma^2\mu}{\alpha_1\beta\eta^2 - \alpha\mu} \leq \epsilon \leq \frac{\alpha_1\eta^2 - \rho}{\rho}. \quad (23)$$

The maximal decay rate  $\sigma_{\max}(\delta)$  is achieved for the closed-loop system system (1)-(2),(7) as the feedback amplifiers are chosen

$$\xi_1 \in [c_1, c_2], \quad \xi_2 \in [c_3, c_4].$$

*Proof.* Observe that to obtain the maximal decay rate (22), it is sufficient to have  $f_1(\xi_1, \epsilon) \geq \frac{1}{\eta}$  and  $f_2(\xi_2, \epsilon) \geq \frac{1}{\eta}$ . Thus,  $f_1(\xi_1, \epsilon) \geq \frac{1}{\eta}$ , i.e.

$$\frac{2\xi_1\alpha_1}{\rho\alpha_1 + (1+\epsilon)\xi_1^2} \geq \frac{1}{\eta},$$

implies that

$$\epsilon \leq h_1(\xi_1) := \frac{2\alpha_1\xi_1\eta - \rho\alpha_1 - \xi_1^2}{\xi_1^2}. \quad (24)$$

Noting that where  $\alpha_1^2\eta^2 - \rho\alpha_1 > 0$  by (10),  $h_1(\xi_1)$  defines an upper bound for  $\epsilon$ , and observe that  $\xi_1$  must be chosen in between the following roots of  $h_1$  to ensure  $\epsilon > 0$  condition is satisfied, see Fig. 2

$$a_1 := \alpha_1\eta - \sqrt{\alpha_1^2\eta^2 - \rho\alpha_1}, \quad a_2 := \alpha_1\eta + \sqrt{\alpha_1^2\eta^2 - \rho\alpha_1}$$

Observe that  $h_1(\xi_1) \geq 0$  if and only if  $\xi_1 \in (a_1, a_2)$ . Seeking the critical points of  $h_1(\xi_1)$

$$\frac{\partial h_1}{\partial \xi_1} = \frac{-2\xi_1^2 \alpha_1 \eta + 2\xi_1 \rho \alpha_1}{\xi_1^4} = 0,$$

leads to  $\xi_1 = \frac{\rho}{\eta}$ . Hence,  $h_1$  achieves its maximum value at  $\xi_1 = \frac{\rho}{\eta}$ . Substituting  $h_1\left(\xi_1 = \frac{\rho}{\eta}\right)$  into (24) yields the following upper bound for  $\epsilon$ :

$$\epsilon \leq \frac{\alpha_1 \eta^2 - \rho}{\rho}. \quad (25)$$

Analogously, by  $f_2(\xi_2, \epsilon) \geq \frac{1}{\eta}$ ,

$$\frac{2\epsilon \xi_2 \alpha_1 \beta}{\epsilon \mu \alpha_1 \beta + (\epsilon \alpha + \gamma^2 \beta) \xi_2^2} \geq \frac{1}{\eta}$$

which implies that

$$\epsilon \geq h_2(\xi_2) := \frac{\beta \gamma^2 \xi_2^2}{2\alpha_1 \beta \xi_2 \eta - \mu \alpha_1 \beta - \alpha \xi_2^2}. \quad (26)$$

Since  $\epsilon > 0$ , the denominator  $2\alpha_1 \beta \xi_2 \eta - \mu \alpha_1 \beta - \alpha \xi_2^2$  is chosen to be strictly positive. This leads to  $\xi_2 \in (a_3, a_4)$  where

$$\begin{aligned} a_3 &:= \frac{\alpha_1 \beta \eta - \sqrt{\alpha_1^2 \beta^2 \eta^2 - \alpha \mu \alpha_1 \beta}}{\alpha} \\ a_4 &:= \frac{\alpha_1 \beta \eta + \sqrt{\alpha_1^2 \beta^2 \eta^2 - \alpha \mu \alpha_1 \beta}}{\alpha}, \end{aligned} \quad (27)$$

$\xi_2 = a_3$  and  $\xi_2 = a_4$  are the two vertical asymptotes of  $h_2(\xi_2)$ , see dashed lines in Fig. 2. Note that this condition ensures  $h_2(\xi_2) \geq 0$ . Seeking the critical points of  $h_2(\xi_2)$

$$\frac{\partial h_2}{\partial \xi_2} = \frac{2\alpha_1 \beta^2 \gamma^2 \eta \xi_2^2 - 2\mu \alpha_1 \beta^2 \gamma^2 \xi_2}{(2\alpha_1 \beta \eta \xi_2 - \mu \alpha_1 \beta - \alpha \xi_2^2)^2} = 0$$

leads to  $\xi_2 = \frac{\mu}{\eta}$ . Hence  $h_2(\xi_2)$  takes its minimum value at  $\xi_2 = \frac{\mu}{\eta}$ . Substituting  $h_2\left(\xi_2 = \frac{\mu}{\eta}\right)$  into (24) yields the following lower bound for  $\epsilon$ :

$$\epsilon \geq \frac{\beta \gamma^2 \mu}{\alpha_1 \beta \eta^2 - \alpha \mu} \quad (28)$$

where  $\alpha_1 \beta \eta^2 - \alpha \mu > 0$  by (10). Restricting  $h_1(\xi_1)$  and  $h_2(\xi_2)$  in between roots and asymptotes, respectively,  $\epsilon$  values corresponding to the filled regions in Fig. 2 satisfy conditions (25) and (28), respectively.

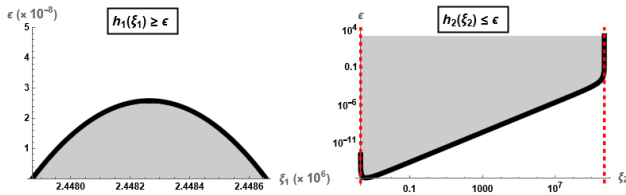


Fig. 2. Considering the realistic material constants in Table I, the upper and lower bounds of  $\epsilon$  depend on  $h_1(\xi_1)$  and  $h_2(\xi_2)$ . Note that the  $h_2$  plot is logarithmic due to the wide ranges of the domain and range.

In order to find ranges of  $\xi_1$  and  $\xi_2$  fix  $\epsilon$  that satisfies (23). The condition  $f_1(\xi_1) \geq \frac{1}{\eta}$ , i.e.

$$-(1 + \epsilon) \xi_1^2 + 2\alpha_1 \eta \xi_1 - \rho \alpha_1 \geq 0,$$

is equivalent to  $\xi_1 \in [c_1, c_2]$ . Analogously, the condition  $f_2 \geq \frac{1}{\eta}$ , i.e.

$$-(\epsilon \alpha + \beta \gamma^2) \xi_2^2 + 2\epsilon \alpha_1 \beta \eta \xi_2 - \epsilon \mu \alpha_1 \beta \geq 0,$$

is equivalent to  $\xi_2 \in [c_3, c_4]$ .

Finally, we prove that such  $\xi_1 \in [c_1, c_2]$  and  $\xi_2 \in [c_3, c_4]$  exist. Note that the sufficient condition for  $[c_1, c_2] \neq \emptyset$  and  $[c_3, c_4] \neq \emptyset$  is the existence of  $\epsilon$  satisfying (23). By (10), there are two cases:

$$\eta = \sqrt{\frac{\rho}{\alpha_1}} + \sqrt{\frac{\mu \gamma^2}{\alpha_1}} \quad \text{or} \quad \eta = \sqrt{\frac{\mu}{\beta}} + \sqrt{\frac{\mu \gamma^2}{\alpha_1}}.$$

Assume  $\eta = \sqrt{\frac{\rho}{\alpha_1}} + \sqrt{\frac{\mu \gamma^2}{\alpha_1}}$ , or in other words,  $\frac{\rho}{\alpha_1} \geq \frac{\mu}{\beta}$ .

$$\frac{\alpha_1 \eta^2 - \rho}{\rho} - \frac{\beta \gamma^2 \mu}{\alpha_1 \beta \eta^2 - \alpha \mu} \geq \frac{\mu \gamma^2}{\rho} + \frac{3\rho \mu \gamma^2}{2\sqrt{\rho^3 \mu \gamma^2}} > 0.$$

Now assume  $\eta = \sqrt{\frac{\mu}{\beta}} + \sqrt{\frac{\mu \gamma^2}{\alpha_1}}$ , or  $\frac{\rho}{\alpha_1} \leq \frac{\mu}{\beta}$ .

$$\frac{\alpha_1 \eta^2 - \rho}{\rho} - \frac{\beta \gamma^2 \mu}{\alpha_1 \beta \eta^2 - \alpha \mu} \geq \frac{\mu \gamma^2}{\rho} + \frac{3\rho \mu \gamma^2}{2\sqrt{\rho^3 \mu \gamma^2}} > 0.$$

Hence,  $\epsilon$  values exist that satisfy (29).  $\square$

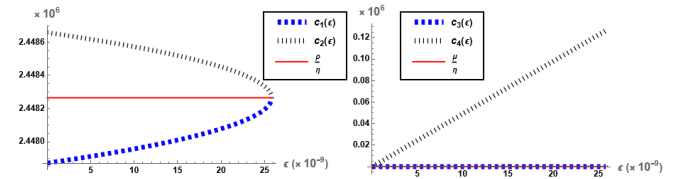


Fig. 3. For the material constants in Table I, graphs of  $c_1, c_2, c_3, c_4$  with respect to  $\epsilon$  satisfying (23).

The amplifier  $\xi_1$  maximizing  $h_1$  and the amplifier  $\xi_2$  minimizing  $h_2$  are always in the respective intervals, i.e.  $\xi_1 = \frac{\rho}{\eta} \in [c_1, c_2]$  and  $\xi_2 = \frac{\mu}{\eta} \in [c_3, c_4]$ . Moreover, as  $\epsilon$  approaches to the upper (lower) bound  $[c_1, c_2]$  gets smaller (larger) and  $[c_3, c_4]$  gets larger (smaller), see Fig. 3. Feedback amplifiers chosen within the intervals ensure that  $f_1(\xi_1, \epsilon) \geq \frac{1}{\eta}$  and  $f_2(\xi_2, \epsilon) \geq \frac{1}{\eta}$  are satisfied, see Fig. 4.

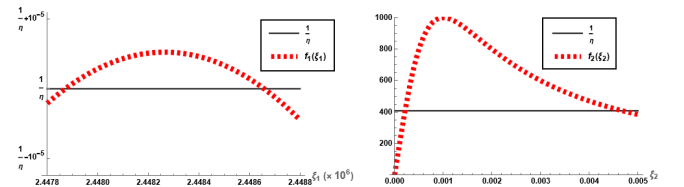


Fig. 4. For the choice of  $\epsilon \approx 10^{-15}$ ,  $f_1(\xi_1), f_2(\xi_2) > \frac{1}{\eta}$  where the maximal decay rate  $\sigma_{\max}$  is obtained for  $\xi_1 \in [c_1, c_2], \xi_2 \in [c_3, c_4]$ .

**Theorem 5. [Case II]** Let  $\epsilon$  be

$$0 < \frac{\beta \gamma^2 \mu}{\alpha_1 \beta \eta^2 - \alpha \mu} \leq \epsilon \leq \frac{\alpha_1 \eta^2 - \rho}{\rho}. \quad (29)$$

Assume that  $[c_1, c_2] \cap [c_3, c_4] \neq \emptyset$  where  $c_1, c_2, c_3, c_4$  are defined in (23). The maximal decay rate  $\sigma_{\max}(\delta_{II})$  is achieved for the closed-loop system (1)-(2),(7) as the feedback amplifier  $\xi_3$  is chosen as the following  $\xi_3 \in [c_1, c_2] \cap [c_3, c_4]$ .

*Proof.* Choosing  $g_1(\xi_3, \epsilon) = f_1(\xi_1 = \xi_3, \epsilon)$  and  $g_2(\xi_3, \epsilon) = f_2(\xi_2 = \xi_3, \epsilon)$ , this case can be seen as a special case of Case I. The rest of the proof works analogously.  $\square$

**Remark III.1.** Note that for the material constants in Table I, Case II does not provide any feedback amplifier  $\xi_3$  to achieve the maximal decay rate  $\sigma_{\max}$ . This may be deduced from Figures 3 and 4 that  $[c_1, c_2] \cap [c_3, c_4] = \emptyset$ . On the other hand, one may have to choose  $\rho$  and  $\mu$  close enough, which is not realistic with piezoelectric material constants, so that the wave propagation speeds get closer, and the maximal decay rate  $\sigma_{\max}$  is obtained, see Fig 5.

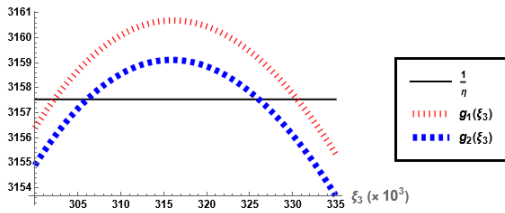


Fig. 5. The choice of  $\rho = \mu = 100$  ensures the existence of  $\xi_3$  such that  $g_1(\xi_3), g_2(\xi_3) > \frac{1}{\eta}$ .

#### IV. SIMULATIONS BY NUMERICAL EXPERIMENTS

Consider a model reduction for (1)-(3) by Finite Differences, as in [9], relying on a direct Fourier filtering technique [1], first proposed by [2].

Letting  $N \in \mathbb{N}$  be given, and defining the mesh size  $h := \frac{1}{N+1}$ , consider a uniform discretization of the interval  $[0, L]$ :  $0 = x_0 < x_1 < \dots < x_i = i * h < \dots < x_N < x_{N+1} = L$ . Now let  $v_j = v_j(t) \approx v(x_j, t)$  and  $p_j = p_j(t) \approx p(x_j, t)$  the approximation of the solution  $(v, p)(x, t)$  of (1)-(3) at the point space  $x_j = j \cdot h$  for any  $j = 0, 1, \dots, N, N+1$ , and  $\vec{v} = [v_1, v_2, \dots, v_N]^T$  and  $\vec{p} = [p_1, p_2, \dots, p_N]^T$ . Now consider the central differences for  $v_{xx}(x_j) \approx (-A_h \vec{v})_j$  and  $p_{xx}(x_j) \approx (-A_h \vec{p})_j$  with the  $N \times N$  matrix  $A_h$  defined by

$$A_h = \frac{1}{h^2} \begin{bmatrix} 2 & -1 & 0 & \dots & \dots & \dots & 0 \\ -1 & 2 & -1 & 0 & \dots & \dots & 0 \\ & & \ddots & \ddots & \ddots & \ddots & \\ 0 & \dots & \dots & 0 & -1 & 2 & -1 \\ 0 & \dots & \dots & \dots & 0 & -1 & 1 \end{bmatrix}. \quad (30)$$

Therefore, the model (1)-(3) is semi-discretized as the following

$$\begin{cases} (C_1 \otimes I) \begin{bmatrix} \ddot{\vec{v}} \\ \ddot{\vec{p}} \end{bmatrix} + (C_2 \otimes A_h) \begin{bmatrix} \vec{v} \\ \vec{p} \end{bmatrix} = 0, \\ v_0 = p_0 = 0, \\ C_2 \begin{bmatrix} v_{N+1} - v_N \\ p_{N+1} - p_N \end{bmatrix} = - \begin{bmatrix} \xi_1 \dot{v}_{N+1} \\ \xi_2 \dot{p}_{N+1} \end{bmatrix}, \quad t \in \mathbb{R}^+ \\ (v, \dot{v})_j(0) = (v^0, v^1)(x_j), \\ (p, \dot{p})_j(0) = (p^0, p^1)(x_j), \quad j = 0, \dots, N+1. \end{cases} \quad (31)$$

where  $\otimes$  is the Kronecker product. Let  $B = \frac{1}{h} \text{tridiag}(0, -1, 1)$  an  $N \times N$  tridiagonal matrix. The discretized energy corresponding to (5) is

$$E_h(t) := \frac{h}{2} \left\{ (C_1 \otimes I) \begin{bmatrix} \dot{\vec{v}}_i \\ \dot{\vec{p}}_i \end{bmatrix} \right\} \cdot \begin{bmatrix} \dot{\vec{v}}_i \\ \dot{\vec{p}}_i \end{bmatrix} + \frac{h}{2} \left\{ (C_2 \otimes B_h) \begin{bmatrix} \vec{v}_i \\ \vec{p}_i \end{bmatrix} \right\} \cdot \left\{ (I \otimes B_h) \begin{bmatrix} \vec{v}_i \\ \vec{p}_i \end{bmatrix} \right\}. \quad (32)$$

Given  $0 \leq \Gamma < 4$ , e the class  $\mathcal{C}_h(\Gamma)$  of filtered solutions of (31) with the filtering parameter  $\Gamma$  is first established in [9] as the following

$$\left\{ \begin{pmatrix} \vec{v} \\ \vec{p} \end{pmatrix} = \sum_{\mu_k^2 h^2 \leq \Gamma} \left[ c_{1k} \begin{pmatrix} \vec{\psi}_k \\ b_1 \vec{\psi}_k \\ \frac{i\mu_k}{\zeta_1} \vec{\psi}_k \\ \frac{i\mu_k b_1}{\zeta_1} \vec{\psi}_k \end{pmatrix} e^{\frac{i\mu_k t}{\zeta_1}} + c_{2k} \begin{pmatrix} \vec{\psi}_k \\ b_2 \vec{\psi}_k \\ \frac{i\mu_k}{\zeta_2} \vec{\psi}_k \\ \frac{i\mu_k b_2}{\zeta_2} \vec{\psi}_k \end{pmatrix} e^{\frac{i\mu_k t}{\zeta_2}} \right] \right\} \quad (33)$$

where  $\mu_k = \sqrt{\lambda_k}$  for  $k > 0$  and  $\mu_{-k} = -\mu_k$ , and  $\lambda_k$  are the eigenvalues of  $A_h$ .

To show the importance of our analysis for the optimal choices of sensor feedback amplifiers, sample numerical simulations are presented for the material constants in Table I. The simulations are considered for  $T_{\text{final}} = 0.1 \text{sec}$  and for  $N = 40$  nodes with  $h = \frac{1}{41} \approx 0.0243$ . In total, three experiment are considered for Case I:

- (I-a) No numerical filtering ( $\Gamma = 4$ ) but optimal feedback amplifiers  $\xi_1 \approx 2.45 \times 10^6$ ,  $\xi_2 \approx 4 \times 10^{-4}$ .
- (I-b) Numerical filtering ( $\Gamma \approx 3.71$ ) with non-optimal feedback amplifiers  $\xi_1 \approx 14, 634$ ,  $\xi_2 \approx 4 \times 10^{-4}$ .
- (I-c) Numerical filtering ( $\Gamma \approx 3.71$ ) optimal feedback amplifiers  $\xi_1 \approx 2.45 \times 10^6$ ,  $\xi_2 \approx 4 \times 10^{-4}$ .

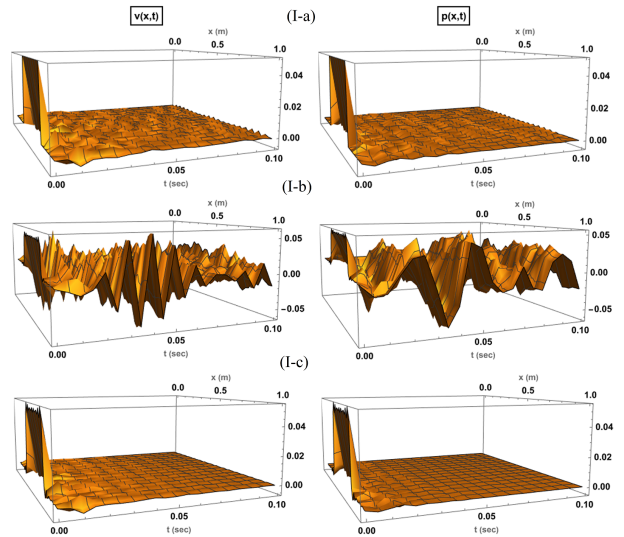


Fig. 6. For Case I, three experiments (I-a),(I-b) and (I-c) show the importance of the filtering and the optimality of sensor feedback amplifiers.

As seen in Figures 6 and 7, for all three cases, highly discontinuous box-type initial conditions are chosen for both initial positions and velocities. For the case (I-a), the optimal amplifiers fail to make it to the maximal decay rate due to spurious high-frequency modes of vibrations. (I-b) By numerically filtering 24 high-frequency eigenvalues, i.e.  $\Gamma \approx 3.71$ , solutions are observed to stabilize faster and the maximal decay rate is achieved. For the case (I-c), even with the same amount of filtering in part (I-b), the maximal decay rate fails to be achieved since the sensor feedback amplifiers are non-optimal. To better show the decay rate the final time is chosen  $T_{\text{final}} = 0.01\text{sec}$  in Fig. 7.

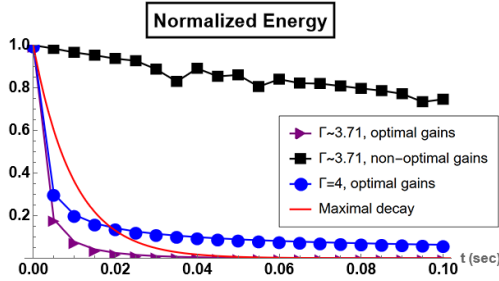


Fig. 7. The energy plots for the numerical experiments (I-a), (I-b), and (I-c) in Fig. 6 to achieve the maximal decay rate  $\sigma_{\text{max}}$ .

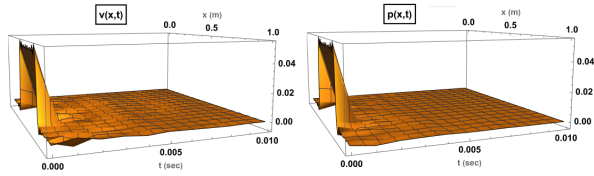


Fig. 8. For Case II, a non-physical case, i.e.  $\rho = \mu = 100$  in Table I with the optimal choice of  $\xi_3 = \frac{\rho}{\eta} = 315, 754$  and the filtering parameter  $\Gamma \approx 3.71$  are chosen. A very fast decay rate is observed.

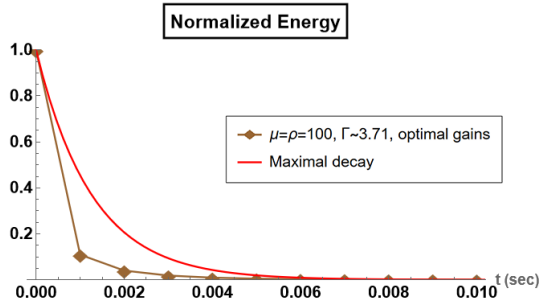


Fig. 9. Normalized energy corresponding to the solutions in Fig. 8 for Case II achieves the maximal decay rate  $\sigma_{\text{max}}$ .

As pointed out in Remark III.1, Case II does not provide any feedback amplifier  $\xi_3$  to achieve the maximal decay rate  $\sigma_{\text{max}}$  for the realistic material constants in Table I. For Theorem 5 to be applicable,  $\mu$  and  $\rho$  must to be sufficiently close. Therefore, we set  $\rho = \mu = 100$  and keep the rest of material constants as in Table I. Now choosing the optimal amplifier  $\xi_3 \approx 315, 754$  with filtering parameter

$\Gamma \approx 3.71$  result in the maximal decay rate, see Figures 8 and 9.

TABLE I  
REALISTIC PIEZOELECTRIC MATERIAL PROPERTIES

| Property               | Symbol   | Value     | Unit              |
|------------------------|----------|-----------|-------------------|
| Length of the beam     | $L$      | 1         | m                 |
| Mass density           | $\rho$   | 6000      | kg/m <sup>3</sup> |
| Magnetic permeability  | $\mu$    | $10^{-6}$ | H/m               |
| Elastic stiffness      | $\alpha$ | $10^9$    | N/m <sup>2</sup>  |
| Piezoelectric constant | $\gamma$ | $10^{-3}$ | C/m <sup>3</sup>  |
| Impermissivity         | $\beta$  | $10^{12}$ | m/F               |

## V. CONCLUSION & FUTURE WORK

In conclusion, the maximal exponential decay rate  $\sigma_{\text{max}}$  together with the optimal sensor feedback amplifiers  $\xi_1, \xi_2, \xi_3$  for the exact (Case I) and simultaneous (Case II) exponential stabilization are obtained analytically so that the system stabilizes to the equilibrium the fastest. It is also analyzed that the results strongly depend on the material constants. Wolfram Demonstrations Projects for the interactive simulation of the vibrational dynamics is already under revision [12]. The next possible project is to apply the ideas here for multi-layer magnetizable beams [5], [6].

Note that the numerical analyses and the proof of exponential stability of the solutions of the model reduction (31) together with the optimal values of feedback amplifiers and the filtering parameter are beyond the scopes of this paper [8]. Thus, they are skipped here.

## REFERENCES

- [1] H.E. Boujaoui, H. Bouslous, L. Maniar, *Boundary Stabilization for 1-d Semi-Discrete Wave Equation by Filtering Technique* Bulletin of TICMI (17-1) 2013, 1–18.
- [2] J.A Infante and E. Zuazua, *Boundary observability for the space semi-discretizations of the 1-D wave equation*, Math. Model. Num. Ann., vol. 33, 1999, pp. 407-438.
- [3] K. Morris, A.Ö. Özer, *Modeling and stability of voltage-actuated piezoelectric beams with electric effect*, SIAM J. Control Optimum, (52-4), 2371-2398, 2014.
- [4] A.Ö. Özer, *Further stabilization and exact observability results for voltage-actuated piezoelectric beams with magnetic effects*, Math. Control Signals Syst., (27), 219-244, 2015.
- [5] A.Ö. Özer, *Modeling and controlling an active constrained layered (ACL) beam actuated by two voltage sources with/without magnetic effects*, IEEE Trans. Automat. Contr., (62-12), 6445–6450, 2017.
- [6] A.Ö. Özer, *Potential formulation for charge or current-controlled piezoelectric smart composites and stabilization results: electrostatic vs. quasi-static vs. fully-dynamic approaches*, IEEE Trans. Automat. Contr., (64-3), 989-1002, 2019.
- [7] A.Ö. Özer, R. Emran, *Revisiting the Direct Fourier Filtering Technique for the Boundary Damped Wave Equation*, under review.
- [8] A.Ö. Özer, R. Emran, A.K. Aydin, *A Robust Model Reduction for the Boundary Feedback Stabilization of Piezoelectric Beams*, in prep.
- [9] A.Ö. Özer, W. Horner, *Uniform boundary observability of Finite Difference approximations of non-compactly-coupled piezoelectric beam equations*, Applicable Analysis, (101-5), 1571-1592.
- [10] A.J.A. Ramos, et al., *Equivalence between exponential stabilization and boundary observability for piezoelectric beams with magnetic effect*, Z. Angew. Math. Phys., (70-60), 2019.
- [11] T. Voss, J.M.A. Scherpen, *Stabilization and shape control of a 1D piezoelectric Timoshenko beam*, Automatica, (47-12), 2780-85, 2011.
- [12] J. Waltherman, A.K. Aydin, A.Ö. Özer, *Piezoelectric beam dynamics*, Wolfram Demonstrations Project, submitted to Wolfram.